Phosphatidylserine (PS) Is Exposed in Choroidal Neovascular Endothelium: PS-Targeting Antibodies Inhibit Choroidal Angiogenesis In Vivo and Ex Vivo

Tao Li,[1,2] Bogale Aredo,[1] Kaiyan Zhang,[1,3] Xin Zhong,[1] Jose S. Pulido,[4] Shusheng Wang,[5] Yu-Guang He,[1] Xianming Huang,[6] Rolf A. Brekken,[6,7] and Rafael L. Ufret-Vincenty[1]

[1]Department of Ophthalmology, University of Texas Southwestern Medical Center, Dallas, Texas, United States
[2]Department of Ophthalmology, Tongji Hospital, Tongji Medical College, Huazhong University of Science and Technology, Wuhan, People's Republic of China
[3]Department of Ophthalmology, Hainan Provincial People's Hospital, Haikou, Hainan, People's Republic of China
[4]Departments of Ophthalmology and Molecular Medicine, Mayo Clinic, Rochester, Minnesota, United States
[5]Departments of Cell and Molecular Biology and Ophthalmology, Tulane University, New Orleans, Louisiana, United States
[6]Department of Pharmacology and the Hamon Center for Therapeutic Oncology Research, University of Texas Southwestern Medical Center, Dallas, Texas, United States
[7]Department of Surgery, University of Texas Southwestern Medical Center, Dallas, Texas, United States

Correspondence: Rafael L. Ufret-Vincenty, Department of Ophthalmology, UT Southwestern Medical Center, 5323 Harry Hines Boulevard, Dallas, TX 75390-9057, USA; Rafael.Ufret-Vincenty@UTSouthwestern.edu.

TL and BA contributed equally to the work presented here and should therefore be regarded as equivalent authors.

Submitted: May 19, 2015
Accepted: September 26, 2015

Citation: Li T, Aredo B, Zhang K, et al. Phosphatidylserine (PS) is exposed in choroidal neovascular endothelium: PS-targeting antibodies inhibit choroidal angiogenesis in vivo and ex vivo. *Invest Ophthalmol Vis Sci*. 2015;56:7137–7145. DOI:10.1167/iovs.15-17302

Purpose. Choroidal neovascularization (CNV) accounts for 90% of cases of severe vision loss in patients with advanced age-related macular degeneration. Identifying new therapeutic targets for CNV may lead to novel combination therapies to improve outcomes and reduce treatment burden. Our goal was to test whether phosphatidylserine (PS) becomes exposed in the outer membrane of choroidal neovascular endothelium, and whether this could provide a new therapeutic target for CNV.

Methods. Choroidal neovascularization was induced in C57BL/6J mice using laser photocoagulation. Choroidal neovascularization lesions costained for exposed PS and for intercellular adhesion molecule 2 (or isolectin B4) were imaged in flat mounts and in cross sections. The laser CNV model and a choroidal sprouting assay were used to test the effect of PS-targeting antibodies on choroidal angiogenesis. Choroidal neovascularization lesion size was determined by intercellular adhesion molecule 2 (ICAM-2) staining of flat mounts.

Results. We found that PS was exposed in CNV lesions and colocalized with vascular endothelial staining. Treatment with PS-targeting antibodies led to a 40% to 80% reduction in CNV lesion area when compared to treatment with a control antibody. The effect was the same as that seen using an equal dose of an anti-VEGF antibody. Results were confirmed using the choroid sprouting assay, an ex vivo model of choroidal angiogenesis.

Conclusions. We demonstrated that PS is exposed in choroidal neovascular endothelium. Furthermore, targeting this exposed PS with antibodies may be of therapeutic value in CNV.

Keywords: choroidal neovascularization, phosphatidylserine, PS-targeting antibody, choroidal angiogenesis, choroidal sprouting, PS-exposure

Age-related macular degeneration (AMD) is a prevalent blinding disease. An estimated 30% of Americans older than 75 years of age have some degree of macular degeneration.[1,2] Furthermore, advanced AMD afflicts approximately 1.8 million individuals in the United States alone.[1] Approximately 90% of severe vision loss in advanced AMD can be attributed to neovascular or "wet" AMD, characterized by the development of pathological angiogenesis originating in the choroid (choroidal neovascularization, CNV).[2] Recent therapeutic advances have led to improvements in clinical outcomes for neovascular AMD,[3] but there remains a significant need for new therapeutic strategies.[4,5] Anti-VEGF therapy has provided significant therapeutic visual benefit, yet it does not decrease the size of the choroidal neovascular complex (it only prevents a further increase in size).[6] Thus, frequent intravitreal injections are needed indefinitely to keep the disease at bay. Targeting different pathways related to the neovascular process may allow for combination therapies that improve clinical success, improve the quality of life, and decrease the treatment burden on patients with "wet AMD."

In normal cells, including vascular endothelium, the aminophospholipid phosphatidylserine (PS) is asymmetrically distributed across the plasma membrane lipid bilayer, such that it is exclusively localized to the membrane's inner leaflet.[7,8] This asymmetry is maintained by enzymes known as aminophospholipid translocases that actively transport PS from the external to the internal leaflet of the plasma membrane.[9,10] On the other hand, the activation of phospholipid scramblases can lead to the loss of the asymmetric distribution of phospholipids in the plasma membrane of cells.[11] Virus-infected cells[12] and, importantly, tumor vascular endothelial cells[13] lose their capacity to maintain PS asymmetry. One

potential trigger for this phenomenon is oxidative stress.[13,14] Phosphatidylserine-targeting antibodies can bind to exposed PS in the outer leaflet of the plasma membrane of tumor vascular endothelium, enabling antibody-dependent cell-mediated cytotoxicity (ADCC).[15] Antibody-dependent cell-mediated cytotoxicity is mediated by monocytes and macrophages and can result in the collapse of the tumor neovasculature.[15]

In this work we propose and test the hypotheses that (1) the abnormal endothelium of choroidal neovascular membranes lacks the ability to maintain PS asymmetry in the plasma membrane lipid bilayer, and (2) PS-targeting antibodies may provide a new therapeutic approach for CNV. We were able to use an in vivo model (laser-induced CNV in mice) to demonstrate that PS is indeed exposed on the neovascular endothelium of CNV. Furthermore, in the laser CNV model and in an ex vivo model (choroidal sprouting assay), we were able to demonstrate that PS-targeting antibodies can inhibit choroidal angiogenesis.

Materials and Methods

Animals

C57BL/6J (Jackson Laboratory, Bar Harbor, ME, USA) mice were used for laser-induced CNV experiments and for the choroidal sprouting assay. Mice were kept in a barrier animal facility at the University of Texas (UT) Southwestern Medical Center under normal lighting conditions with 12-hour-on/12-hour-off cycles. All applicable international, national, and institutional guidelines for the care and use of animals, including the National Institutes of Health (NIH) Guide for the Care and Use of Laboratory Animals and the ARVO Statement for the Use of Animals in Ophthalmic and Vision Research, were followed. All experiments were approved by the UT Southwestern Medical Center Institutional Animal Care and Use Committee (IACUC). Before all procedures, animals were anesthetized one at a time with a ketamine-xylazine cocktail (100 mg/kg ketamine, 5 mg/kg xylazine).

Antibodies

All antibodies were dissolved in PBS. The PS-targeting antibodies that were used in this study were 1N11 (a fully human antibody, also known as PGN635; used only for in vivo staining of PS),[16] mch1N11 (a murine IgG2a chimeric version of 1N11),[17] and mch11.31 (a murine IgG2a chimeric version of 11.31, which is a fully human antibody, also known as PGN632).[18] These antibodies were generated by phage display technology and were selected based on specificity for PS. The binding of mch1N11 to PS, similar to what has been found with other PS-targeting antibodies like 2aG4, 3G4, and bavituximab, is dependent on β2-glycoprotein-1. Bavituximab and 2aG4 have the same Fv region, while mch1N11 and PGN635 (1N11) share another Fv region.[17] Biacore experiments have revealed that bavituximab binds to human β2-glycoprotein-1 with an affinity of 1.7×10^{-8} M (monovalent interaction) and an avidity of $\sim 10^{-10}$ M (divalent interaction).[19] In contrast, the binding of PGN632 and mch11.31 to PS is independent of β2-glycoprotein-1, and thus they were not included in those studies. All PS-targeting antibodies were provided by Peregrine Pharmaceuticals, Inc. (Tustin, CA, USA). The positive control antibody, r84 (an anti-VEGF antibody,[20] generously supplied by Affitech, Inc., Oslo, Norway), was used for the intraperitoneal (IP) experiments. The negative control antibodies used in this study were C44 (mouse IgG2a control used for CNV inhibition experiments) and "control IgG" (human IgG control used for staining experiments).

Binding of PS-Targeting Antibodies to Plastic-Immobilized Phosphatidylserine

Binding of the PS-targeting antibodies mch1N11 and mch11.31 to PS was measured using an ELISA protocol as described previously.[21] Briefly, PS was dissolved in *n*-hexane to a concentration of 50 μg/mL, and 100 μL of this solution was added to wells of 96-well plates (Immulon-1B microtiter plates; Dynex, Chantilly, VA, USA). After evaporation of the solvent in air, the plates were blocked for 2 hours with 10% fetal bovine serum (FBS) diluted in Dulbecco's PBS. The plates were then incubated with the primary antibodies diluted in Dulbecco's PBS containing 2 mmol/L $Ca2^{+}$ in the presence of 10% FBS for 2 hours at room temperature. After washing, the antibodies were detected using a horseradish peroxidase–conjugated goat anti-mouse secondary antibody (1:1000). The chromogenic substrate *o*-phenylenediamine dihydrochloride was used, and plates were read at 490 nm using a microplate reader (Molecular Devices, Palo Alto, CA, USA). Each antibody dilution was run in duplicate.

Laser Induction of CNV and Treatment With PS-Targeting Antibodies

The pupils of anesthetized 2- to 6-month-old C57BL/6J mice were dilated using one drop per eye of a tropicamide 1% solution (Alcon Laboratories, Inc., Fort Worth, TX, USA) 5 minutes before laser application. Gonak (2.5% hypromellose solution; Akorn, Inc., Lake Forest, IL, USA) was applied to both eyes, and the eyes were imaged with a Micron III murine fundus camera (Phoenix Research Laboratories, Pleasanton, CA, USA). Laser was delivered using an Iridex Oculight GL 532-nm diode laser (Mountain View, CA, USA) connected to the Micron III using a laser injector (Phoenix Research Laboratories, Pleasanton, CA, USA). The original Micron III laser injector system delivered approximately 15% of the energy to the eye, so the laser energy was adjusted accordingly. The parameters used to reproducibly obtain successful laser spots (as confirmed by a gas bubble formation indicating rupture of Bruch's membrane) were 1100 mW, 100 ms, and 50-μm spot size for the early experiments. Improvements in the delivery system by Phoenix Research Laboratories led to increased laser energy delivery, and thus the parameters for the optimized treatment protocol were 280 mW, 100 ms, and 50-μm spot size. In all cases, four laser spots were applied, 2 to 3 disc diameters from the optic nerve at roughly the 12, 3, 6, and 9 o'clock positions.

As a guideline for dosing in the experiments involving treatment, we referred to the experiments in mouse tumors done by Thorpe's laboratory, with modifications based on the number of injections.[21] Mice were injected with 250 μg IP of either the PS-targeting antibodies (mch1N11 or mch11.31), control antibody C44, or anti-VEGF antibody r84. For the early treatment experiments, injections were given on days 5 and 7 after laser, and eyes were collected 14 days after laser. For the optimized treatment approach, PS-targeting antibodies were injected on days 2, 4, and 6 post laser, and eyes were collected 8 days after laser.

Staining for ICAM-2 and PS Exposure

Phosphatidylserine exposure on vasculature was evaluated by in vivo localization via intravenous injection of PS-targeting antibody 1N11 before collection of the eyes.[16] This avoids staining the PS that is normally present on the inner leaflet of plasma membranes. Mice received 100 μg 1N11 or control IgG by tail vein injection. One hour later, mice were anesthetized and perfused with heparinized PBS by intracardiac injection,

Investigative Ophthalmology & Visual Science

and eyes were collected and fixed in 4% paraformaldehyde for 30 minutes at room temperature (RT). Flat mounts were prepared as previously described.[22] Briefly, the samples were postfixed for 1 hour, incubated with blocking buffer (PBS with 0.5% Triton X-100 and 5% goat serum), and stained with a 1:500 dilution rat anti-intercellular adhesion molecule 2 (anti-ICAM-2, BD Pharmingen, San Jose, CA, USA) at 4°C overnight. After washing and applying secondary antibodies (1:200 dilution of AF488 goat anti-rat and 1:200 dilution of AF594 goat anti-human; both from Invitrogen, Inc., Grand Island, NY, USA), the samples were flat mounted on glass slides and imaged using a Zeiss AxioObserver (Zeiss, Inc., Thornwood, NY, USA) motorized wide-field epifluorescence microscope equipped with a Hamamatsu Orcall-BT-1024G (Hamamatsu Corporation, Middlesex, NJ, USA) monochrome camera and fluorescence filter sets for FITC, Texas Red, and CY7.

Quantification of CNV

Flat mounts were prepared, stained, and imaged as described above. For CNV area quantification, images of ICAM-2-stained CNV lesions were measured using ImageJ software (http://imageJ.nih.gov/ij/index.html; provided in the public domain by the National Institutes of Health, Bethesda, MD, USA). In our experience,[23] anti-ICAM-2 staining results in the best visualization of the vasculature in CNV lesions (compared to a PECAM-1 antibody, isolectin B4, and FITC-dextran), which is consistent with the thorough study by Campa et al.[24] This allowed us to include and measure only areas demonstrating a vascular pattern on ICAM-2 staining. Measurements and quantification were performed by a masked investigator. The results were reported as CNV area normalized to the C44 control (referred to by others[25–28] as "relative CNV size").

Immunohistochemistry of Retinal Paraffin Sections

Eight days after laser injury, mice received 100 μg human 1N11 (primary antibody) or control IgG by tail vein injection. One hour later, mice were anesthetized, then perfused with heparinized PBS by intracardiac injection, and eyes were collected for quick freeze followed by freeze substitution as described previously.[29] Briefly, eyes were immediately placed in 2-mL tubes, frozen in liquid nitrogen-cooled isopentane for 2 minutes followed by liquid nitrogen, and freeze substituted in methanol/acetic acid (97:3) in a –80°C freezer for at least 48 hours. After gradually warming to RT (–20°C for 24 hours, 4°C for 4 hours, then RT), the eyes were transferred to 100% ethanol for paraffin embedding using routine methods. The paraffin blocks were cut (6-μm sections) across the laser lesion, deparaffinized, and rehydrated in xylene and graded ethanol. Sections were then blocked and vessels were stained with a 1:100 dilution of FITC-labeled isolectin B4 (IB4; Vector Labs, Burlingame, CA, USA). Isolectin B4 stains endothelial cells, unmyelinated neurons, and microglia. To detect 1N11, a 1:200 dilution of AF594 goat anti-human antibody (Invitrogen) was used. The lesion spots were imaged as described previously.[29]

Choroid Sprouting Assay

Eyes from 5-week-old mice were enucleated and kept on ice-cold medium (Dulbecco's modified Eagle's medium [DMEM]/F-12; 1:1) for a few minutes, and the anterior segment was dissected out. The RPE-choroid-sclera (choroid) was separated from the retina, and the peripheral tissue was cut into approximately 0.5- × 0.5-mm pieces as previously described by Shao et al.[30] The choroid pieces were placed in Matrigel (35 μL/well), seeded in 24-well plates, and kept for 7 days in a cell culture incubator (37°C and 5% CO_2) under the following conditions: (1) VEGF 50 μg/mL, (2) no treatment in the first 24 hours, (3) medium changed every 3 days, and (4) the antibodies (mch1N11 versus control C44) applied (10 μg/mL) on days 3 and 5. On day 7, phase-contrast photos of individual pieces were taken. The area of sprouting and the maximal extension of angiogenesis from the choroidal tissue edge were then measured by a masked investigator using ImageJ computer software (http://imageJ.nih.gov/ij/index.html).

Statistical Analysis

SigmaPlot 11.0 (Systat Software, Inc., San Jose, CA, USA) and Microsoft Excel (Redmond, WA, USA) were used for statistical analysis. Data are presented as the mean ± standard error of mean (SEM). A two-tailed Student's *t*-test was performed when comparing two groups. A one-way analysis of variance (ANOVA) followed by a Tukey test was applied when comparing more than two groups. A P value < 0.05 was considered significant.

Results

Binding of Phosphatidylserine-Targeting Antibodies to PS

Binding of the PS-targeting antibodies mch1N11 and mch11.31 was tested by ELISA, using plates that had been coated with PS. As a positive control we used the PS-targeting antibody 2aG4, which has been well characterized previously.[31,32] As a negative control we used C44 (mouse IgG2a control). All of the antibodies in this assay are of the IgG2a isotype. The binding of both mch1N11 and mch11.31 to PS was very similar to that of 2aG4 (Fig. 1), indicating that they have similar binding affinities. The calculated half maximal effective concentration (EC50) values for binding were 0.15 nM for mch1N11, 0.17 nM for mch11.31, and 0.14 nM for 2aG4 (Fig. 1b). As previously reported, bavituximab and 2aG4 share the same Fv region and have a Kd for PS of 10^{-10} M.[33]

Phosphatidylserine Is Exposed in Laser-Induced Choroidal Neovascularization

To test the hypothesis that PS is exposed in the outer leaflet of the cell membrane in the neovascular endothelium of CNV, we induced CNV in C57BL/6J mice using the laser photocoagulation model. On day 8 post laser, double immunostaining was performed for exposed PS and for ICAM-2. The first primary antibody (1N11 versus control human IgG) was administered by intravenous injection 1 hour before perfusing the mice and collecting the eyes. The second primary antibody was applied after preparing the flat mounts (ICAM-2) or retinal sections (IB4).

Laser photocoagulation led to the formation of robust vascular complexes (CNV) that stained positive for ICAM-2. Figure 2a shows an example of an ICAM-2-stained lesion, and Figure 2d shows another lesion under higher magnification. These vessels also stained strongly for PS (Figs. 2b, 2e). There was a high degree of colocalization of staining for the ICAM-2 and PS antibodies (Figs. 2c, 2f), indicating that the PS exposure was occurring in the vascular endothelium of the CNV lesions. There was very low nonspecific staining using this technique, as demonstrated by the lack of staining of CNV when mice were injected with control IgG instead of the PS-targeting antibody (compare Figs. 2g, 2h).

Investigative Ophthalmology & Visual Science

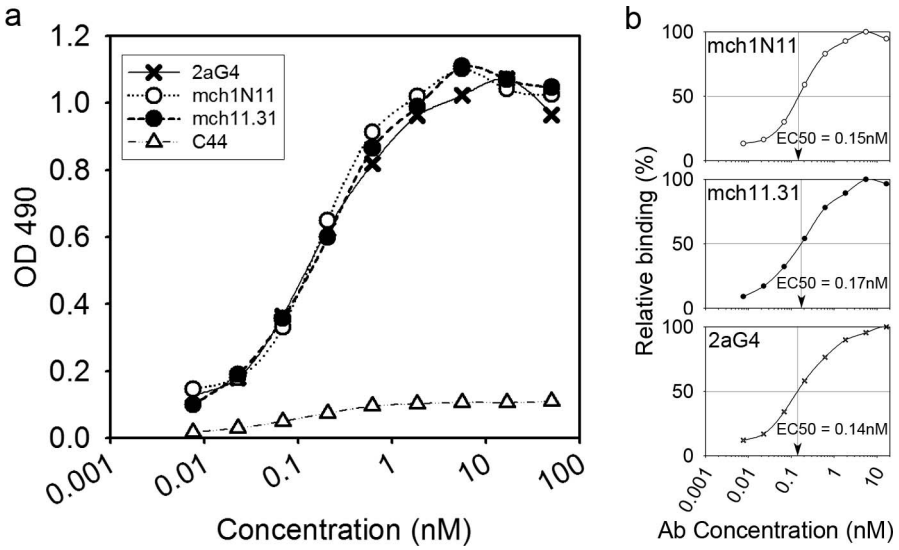

Figure 1. Binding of mch1N11 and mch11.31 to PS. (**a**) Binding of the PS-targeting antibodies mch1N11 and mch11.31 to PS-coated microplates was measured in comparison to the positive control 2aG4 and the negative control C44. PS-coated microtiter plates were exposed to the antibodies at concentrations ranging from 0.0076 to 50 nM. The bound antibody was detected using goat anti-mouse IgG-horseradish peroxidase. The experiment was done in duplicate. The graph represents one of two experiments with similar results. (**b**) EC50 values for binding were calculated separately for mch1N11, mch11.31, and 2aG4.

In order to confirm the colocalization of PS staining with another vascular marker (IB4), and also to determine if normal retinal vasculature demonstrated exposure of PS, lasered eyes were collected for paraffin embedding 1 hour after intravenous injection with 1N11, and CNV lesions were imaged in retinal cross sections (Fig. 3). Immunohistochemistry (IHC) of these sections confirmed that PS exposure was present on the choroidal neovascular complex (Figs. 3a–3c, arrows), but not in normal retinal vasculature (arrowheads). An area of staining is also observed in the choroid directly under the CNV, which may be due to apoptosis in the choroid after laser treatment as reported by others.[34] Retinal apoptosis has also been documented after laser application.[35] However, this section is likely toward the edge of a laser lesion, where there are CNV and significant effects on the choroid but minimal changes in the retina itself. Another area outside of a laser lesion was imaged (Figs. 3d–3f) and demonstrated good IB4 staining (Fig. 3d) of retinal (arrowheads) and choroidal vessels, but no staining when using the PS-targeting antibody 1N11 (Fig. 3e).

PS-Targeting Antibodies Lead to a Reduction in CNV Size

Having shown that PS is indeed exposed in the vascular endothelium of CNV and not in normal retinal vasculature, we then tested whether PS-targeting antibodies would have an effect in CNV formation and growth. A dose–response experiment using PS-targeting antibody mch1N11 given IP demonstrated that a good inhibitory effect on CNV could be seen with a dose of PS-targeting antibody of 250 μg (Fig. 4). Combining mch1N11 and the anti-VEGF antibody r84 did not seem to increase the inhibitory effect. However, it should be noted that the doses of mch1N11 and r84 used in this experimental group were only 125 μg/mouse each (to control for the total amount of antibody, which was 250 μg for the negative control). This dose (at least for mch1N11) may be too low, based on the results of the rest of this experiment. Future experiments will need to be done to

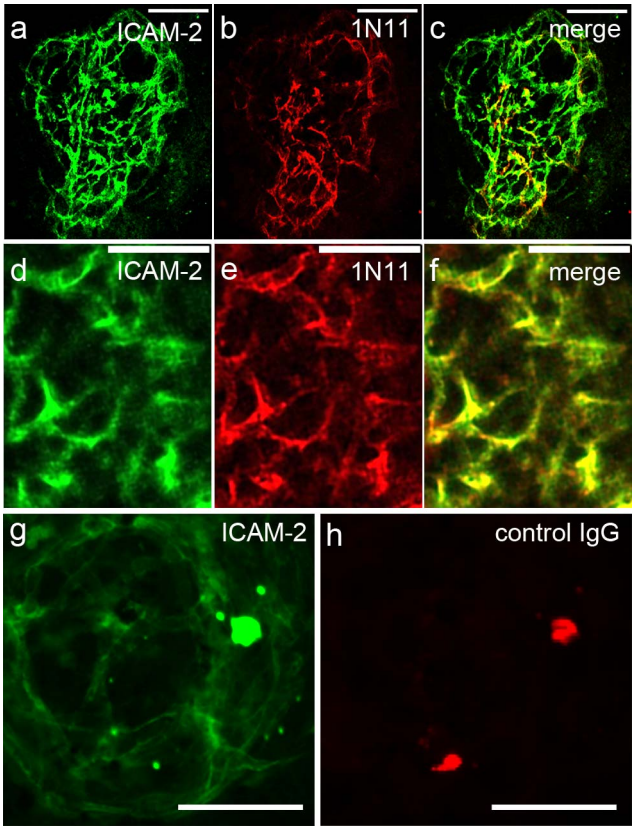

Figure 2. Immunostaining of flat mounts with PS-targeting antibodies demonstrates that PS is exposed on neovascular endothelium and colocalizes with anti-ICAM-2 staining of CNV. (**a–f**) Representative images of two different CNV lesions stained for ICAM-2 (**a**, **d**) and exposed PS (**b**, **e**). The red and green channels were merged (**c**, **f**) and demonstrate a high degree of colocalization of PS and ICAM-2. Another lesion was costained with ICAM-2 (**g**) and with control IgG (**h**). The lack of signal when the control IgG was used demonstrates that the background is very low. A few artifacts are seen (*horizontal line* in [**e**, **f**] and *bright spots* in [**g**, **h**]). *Scale bars*: 100 μm (**a–c**, **g**, **h**); 50 μm (**d–f**).

Investigative Ophthalmology & Visual Science

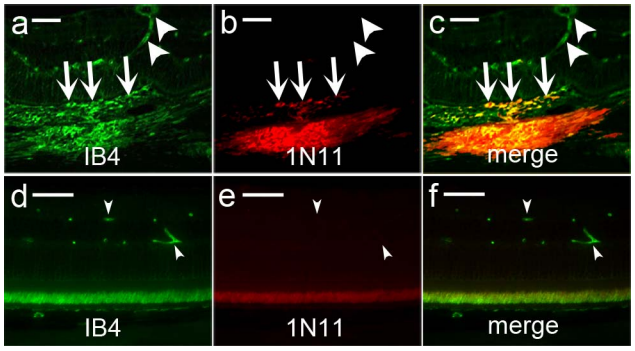

Figure 3. Immunohistochemistry of retinal cross sections of 6-month-old B6 mice (**a**–**c**) shows that PS exposure was present on the choroidal neovascular complex (*arrows*), but not in normal retinal vasculature (*arrowheads*). The merged image (**c**) shows areas of double staining for IB4 and PS in *yellow*; this is seen only in the choroidal neovascular complex and the underlying choroid. An area away from a laser spot was also imaged (**d**–**f**) and shows staining of retinal and choroidal vessels with IB4 (**d**). Yet there is no PS staining of this normal vasculature (**e**, **f**). *Scale bars*: 50 μm.

explore if there is any synergistic effect from combining PS inhibition and VEGF inhibition at higher doses. Separate experiments (data not shown) suggested that for the PS-targeting antibody mch11.31, a dose of 250 μg was also ideal for efficacy. Thus, to corroborate the effect of PS-targeting antibodies on CNV formation, further experiments used a dose of 250 μg.

Eyes were lasered and mice were then treated with the two different PS-targeting antibodies (mch11.31 and mch1N11). These were given IP on days 5 and 7 after laser-induced injury. In two separate experiments, mch11.31 led to an average reduction in CNV area of 61% compared to C44 (Figs. 5a, 5b; $P = 0.038$ and $P = 0.006$, respectively). Antibody mch1N11 also led to a 58% reduction in CNV area (Fig. 5b; $P = 0.003$).

Small exploratory experiments suggested that CNV formation (ICAM-2 staining) and PS exposure start as early as 2 days after the laser, but that pretreatment with PS-targeting antibodies 2 hours before laser induction did not result in any CNV reduction (data not shown). Our results suggested that CNV reached maximum size at around days 8 to 10, consistent with observations by other groups who described a maximum size at days 5 to 10.[36–38] In the experiments shown in Figures 5a and 5b, we treated mice toward the end of the growth phase of the CNV (days 5 and 7). We designed an optimized protocol that would involve treating mice systemically at early, intermediate, and late time points (days 2, 4, and 6) within the CNV growth phase. Another modification was to collect the eyes near the peak of the CNV size (day 8) to allow for good CNV growth while avoiding potential issues with early spontaneous regression of the lesions. Following this protocol (Fig. 5c), we observed a substantial inhibition of CNV growth with the PS-targeting antibody (mch1N11) when compared to the control antibody C44 (Fig. 5d). A statistically significant reduction in CNV area (~80% reduction) was seen ($P < 0.001$). No difference was observed between the PS-targeting antibody and the anti-VEGF antibody r84, which was used as positive control (Fig. 5d, $P = 0.98$). Representative lesions are shown in Figures 5e through 5g.

PS-Targeting Decreased Choroidal Angiogenesis in an Ex Vivo Model

There is no ideal animal model for the CNV that occurs in AMD and other eye diseases. Thus, it was relevant to test whether the effect of PS targeting on choroidal angiogenesis was a phenomenon isolated to the laser CNV model or if it could be reproduced in a different model. The ex vivo model of choroid sprouting developed in Smith's laboratory[30] has been shown to be a reproducible model of choroidal angiogenesis, where treatment effects can be accurately assessed. The sprouts are tube-like growths consisting of endothelial cells surrounded by pericytes.[30] Of particular interest, Shao et al.[30] demonstrated that there is a large number of $CD68^+$ monocyte/macrophages in choroidal sprouts. Using this model, we were able to demonstrate a significant inhibition of angiogenesis by the PS-targeting antibody mch1N11 versus C44 (Fig. 6). There was a reduction in the area of choroid sprouting (Fig. 6c, $P < 0.05$) and also in the longest vessel growth (Fig. 6d, $P < 0.05$).

Discussion

Our objective in this work was to determine whether the vasculature in CNV demonstrates exposure of PS, and if so, whether this could provide a new target for therapeutic intervention. The asymmetric distribution of phospholipids in the plasma membrane and the phenomenon of PS exposure were first described in the 1970s in relation to platelet activation.[39,40] Phosphatidylserine exposure also occurs in apoptotic cells[41] and is the basis for the Annexin V test for apoptosis.[42,43] It may also be associated with oxidative stress,[13,14] aging,[44] and viral infections.[15,45] Phosphatidylserine exposure has also been well characterized in tumor vasculature in the absence of apoptosis.[13] In endothelial cells, PS exposure can be triggered by hypoxia/reoxygenation, acidity, thrombin, inflammatory cytokines, and hydrogen peroxide.[7] All of these triggers can lead to PS exposure in the absence of necrosis or apoptosis.[7] Many of these stressors are known to be present both in the laser model of CNV and also in neovascular AMD.

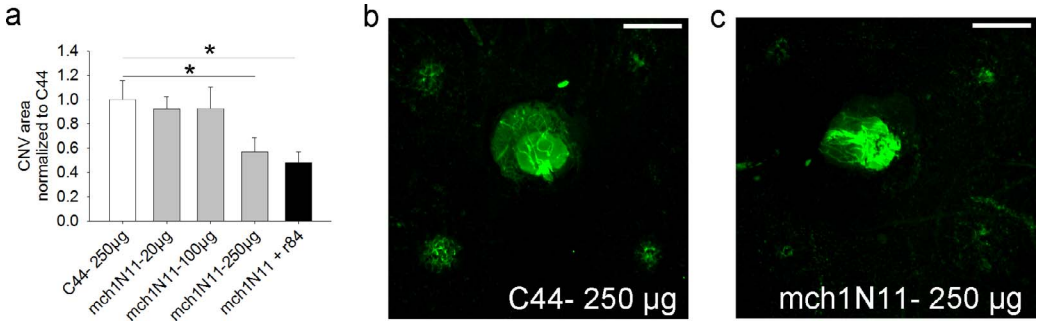

Figure 4. Dose–response experiment for inhibition of laser-induced CNV by PS-targeting antibody mch1N11. (**a**) Doses of 20, 100, and 250 μg of mch1N11 were tested in 2-month-old B6 mice, and inhibition was seen at the 250-μg dose. (**b**, **c**) Examples of flat mounts of mice treated with either 250 μg C44 (negative control [**b**]) or 250 μg mch1N11 (**c**) are shown. $n = 4$ mice/group, *scale bar*: 250 μm.

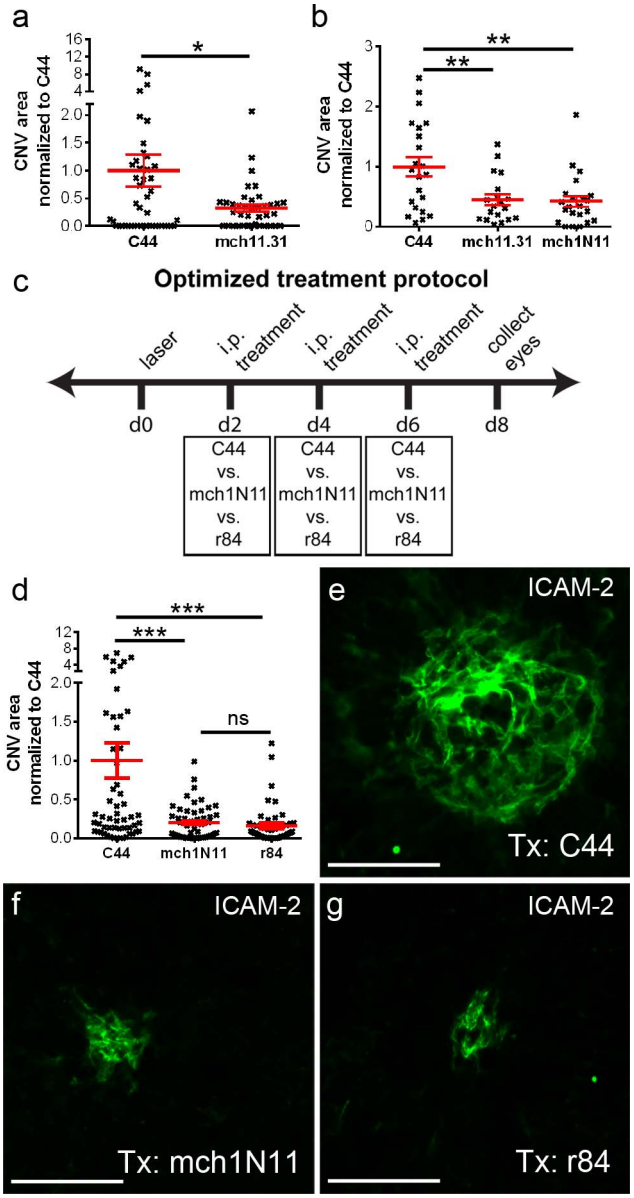

Figure 5. PS-targeting antibodies administered intraperitoneally inhibit laser-induced CNV. In two separate experiments, quantification of CNV area 14 days after laser demonstrates that PS-targeting antibodies cause a decrease in CNV size (**a**, **b**). The CNV area was normalized to the negative control C44. (**a**) After IP injection (days 5 and 7 after laser), the monoclonal PS-targeting antibody mch11.31 causes a significant reduction in CNV area compared to control antibody C44 ($n = 6$ mice/group). (**b**) Both murine chimeric PS-targeting antibodies mch11.31 and mch1N11 cause a similar reduction in CNV area when given IP on days 5 and 7 after laser compared to C44 ($n = 3$ mice/group). (**c**) Schematic representation of an optimized experimental protocol. In essence, mice were treated with either C44 (negative control), mch1N11 (PS-targeting antibody), or r84 (anti-VEGF antibody) on days 2, 4, and 6 after laser. The eyes were collected on day 8, and the flat mounts were stained with ICAM-2 for CNV measurements. (**d**) Compared to C44, CNV area is significantly reduced after mch1N11 treatment, and this effect is similar to that seen with the anti-VEGF antibody r84 ($n = 7$ mice/group). Representative images are shown for ICAM-2 staining of the CNV lesions in mice treated with control antibody C44 (**e**), PS-targeting antibody mch1N11 (**f**), and anti-VEGF antibody r84 (**g**). In these CNV images the antibody used for staining is shown in the *upper right-hand corner*, while the antibody used for treatment (Tx) is shown in the *lower right-hand corner*. $^{*}P < 0.05$; $^{**}P < 0.01$; $^{***}P < 0.001$; *scale bars*: 100 μm.

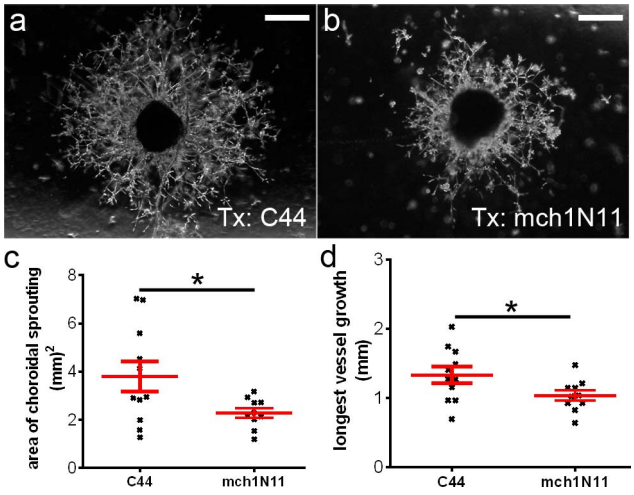

Figure 6. Choroid sprouting assay demonstrating the inhibitory effect of a PS-targeting antibody on the growth of choroidal vessels in Matrigel. Choroid pieces (RPE-choroid-sclera from peripheral retina of 5-week-old mice) were seeded into 24-well plates containing Matrigel, incubated in VEGF-containing medium, and treated with PS-targeting antibody (mch1N11) or control (C44) on days 3 and 5. The antibody used for treatment (Tx) is shown in the *lower right-hand corner* of each choroidal sprouting image. There is extensive choroidal angiogenesis when the tissue is incubated with control antibody C44 (**a**). The PS-targeting antibody mch1N11 significantly reduced the choroidal sprouting (**b**). Quantitation of the area of sprouting (**c**) and the maximal extension of angiogenesis from the choroidal tissue edge (**d**) demonstrate a significant decrease in the PS-targeting antibody group when compared to control. The number of choroidal pieces in each experimental group is shown (n). $^{*}P < 0.05$; *scale bars*: 500 μm.

Using a modified IHC technique (intravenous injection of a PS-targeting antibody that was used as a primary antibody for IHC) we demonstrate that, similar to tumor vasculature, PS is exposed in the endothelium of CNV. A recent study by Morohoshi et al.[46] showed that antibodies to PS are elevated in the serum of patients with AMD, and particularly in those with CNV.[46] Our observation of exposed PS in choroidal neovascular endothelium, in combination with the findings by Morohoshi et al.,[46] would suggest that PS exposure is a relevant phenomenon in neovascular AMD. We propose that whenever CNV develops, the new endothelial cells in CNV are "immature" and have increased exposure of PS leading to the generation of antibodies against this neoantigen.

In the setting of cancer, the body produces endogenous antibodies against tumors that can be used for diagnosis but are not effective in coping with the tumor.[47–49] Similarly, endogenous antibodies against PS are not effective in controlling CNV. Endogenous anti-PS antibodies may be inefficient in causing the destruction/regression of the CNV due to relatively low levels and/or inefficient induction of complement-dependent cytotoxicity or ADCC. Of note, in the Morohoshi et al.[46] study, even though the correlation with neovascular AMD was high for anti-PS antibodies, the actual level of the anti-PS antibodies was one of the lowest, roughly 1/25th of the concentration of the highest autoantibodies detected in all patients. In the case of tumors, administration of monoclonal antibodies[50,51] directed against the same targets recognized by the endogenous antibodies can be of therapeutic value. We propose that a similar approach, administering exogenous PS-targeting monoclonal antibodies, may be of benefit to neovascular AMD patients.

The potential use of PS-targeting antibodies for therapeutic purposes in tumors was introduced in the last decade.[7,16,52] Targeting of PS has been shown to cause tumor regression in animal models.[31] Also, a phase II clinical trial in lung cancer patients using a PS-targeting antibody in combination therapy has suggested efficacy,[53] and randomized phase III trials are now in progress. However, our investigation of PS exposure in CNV and the potential use of PS-targeting antibodies for its treatment is novel. Our experiments showed that injecting PS-targeting antibodies led to a significant reduction in CNV size. Furthermore, we could corroborate the results using two different PS-targeting antibodies. The degree of CNV inhibition induced by the PS-targeting antibodies was comparable to that obtained with the use of an anti-VEGF antibody. Finally, the efficacy was also similar to that reported by others for anti-VEGF therapies using the laser-induced CNV model.[23,54,55]

Laser photocoagulation is the most widely used animal model of experimental CNV. Still, we decided to test whether our results could be reproduced in another useful model of choroidal angiogenesis. We used an ex vivo model of choroidal angiogenesis that is amenable to therapeutic tests: the choroid sprouting assay, in which there is ex vivo growth of choroidal vascular endothelial tubes with surrounding pericytes and macrophages.[30] The data from the choroid sprouting assay confirmed that PS-targeting antibodies are effective in inhibiting choroidal angiogenesis, suggesting that the observed effects are due to the specific targeting of the neovascular endothelium.

Our findings of increased PS exposure in CNV and a therapeutic effect of PS-targeting antibodies raise a whole new set of questions. Future studies will be centered on exploring the mechanism of action of PS-targeting antibodies in CNV. One proposed mechanism of action of PS-targeting antibodies in tumors is by attracting macrophages and inducing ADCC.[15] More work is needed to determine if ADCC is in fact involved in the inhibition of CNV growth. Furthermore, other potential mechanisms should be explored. For example, the Thorpe laboratory recently reported that exposed PS can directly exert an immunosuppressive effect in the tumor microenvironment by shifting the balance of cytokines in the tumor microenvironment from immunosuppressive to immunostimulatory.[31] The fact that both laser-induced CNV lesions[56,57] and also choroidal sprouts[30] have abundant associated monocytes/macrophages/microglia is consistent with a possible role of these cells in the mechanism of action of PS-targeting antibodies. We also plan to explore the potential use of PS-targeting antibodies in other forms of ocular angiogenesis and as part of combination therapies. Candidates for a combination approach with PS-targeting antibodies include anti-VEGF agents and radiation therapy[32,58] (which increases the exposure of PS in tumor vasculature).[32] Finally, in general, PS becomes exposed due to either a decrease in activity of a translocase[59] or an increase in activity of a scramblase.[60] It would be useful to explore if there is any specific translocase that becomes inactive, or scramblase that is activated in neovascular endothelium and that could explain the development of PS exposure in these cells.

Acknowledgments

Supported by National Institutes of Health Visual Science Core Grant EY020799, an unrestricted grant from Research to Prevent Blindness, a grant from the David M. Crowley Foundation, the Patricia and Col. William Massad Retina Research Fund, the Charles Y.C. Pak Retina Research Fund, and a Hainan Provincial Social Development Special Fund for Science and Technology.

Disclosure: **T. Li**, None; **B. Aredo**, None; **K. Zhang**, None; **X. Zhong**, None; **J.S. Pulido**, None; **S. Wang**, None; **Y.-G. He**, None; **X. Huang**, None; **R.A. Brekken**, Peregrine Pharmaceuticals (F); **R.L. Ufret-Vincenty**, None

References

1. Friedman DS, O'Colmain BJ, Muñoz B, et al. Eye Diseases Prevalence Research Group: prevalence of age-related macular degeneration in the United States. *Arch Ophthalmol*. 2004; 122:564–572.
2. Congdon N, O'Colmain B, Klaver CC, et al. Causes and prevalence of visual impairment among adults in the United States. *Arch Ophthalmol*. 2004;122:477–485.
3. Kim LA, D'Amore PA. A brief history of anti-VEGF for the treatment of ocular angiogenesis. *Am J Pathol*. 2012;181:376–379.
4. Schmidt-Erfurth U, Chong V, Loewenstein A, et al. European Society of Retina Specialists: guidelines for the management of neovascular age-related macular degeneration by the European Society of Retina Specialists (EURETINA). *Br J Ophthalmol*. 2014;98:1144–1167.
5. Haller JA. Current anti-vascular endothelial growth factor dosing regimens: benefits and burden. *Ophthalmology*. 2013; 120:S3–S7.
6. Kaiser PK, Blodi BA, Shapiro H, Acharya NR; MARINA Study Group. Angiographic and optical coherence tomographic results of the MARINA study of ranibizumab in neovascular age-related macular degeneration. *Ophthalmology*. 2007;114: 1868–1875.
7. Ran S, Thorpe PE. Phosphatidylserine is a marker of tumor vasculature and a potential target for cancer imaging and therapy. *Int J Radiat Oncol Biol Phys*. 2002;54:1479–1484.
8. Williamson P, Schlegel RA. Back and forth: the regulation and function of transbilayer phospholipid movement in eukaryotic cells. *Mol Membr Biol*. 1994;11:199–216.
9. Devaux PF. Protein involvement in transmembrane lipid asymmetry. *Annu Rev Biophys Biomol Struct*. 1992;21:417–439.
10. Balasubramanian K, Schroit AJ. Aminophospholipid asymmetry: a matter of life and death. *Annu Rev Physiol*. 2003;65: 701–734.
11. Kodigepalli KM, Bowers K, Sharp A, Nanjundan M. Roles and regulation of phospholipid scramblases. *FEBS Lett*. 2015;589: 3–14.
12. Soares MM, King SW, Thorpe PE. Targeting inside-out phosphatidylserine as a therapeutic strategy for viral diseases. *Nat Med*. 2008;14:1357–1362.
13. Ran S, Downes A, Thorpe PE. Increased exposure of anionic phospholipids on the surface of tumor blood vessels. *Cancer Res*. 2002;62:6132–6140.
14. Toyokuni S, Okamoto K, Yodoi J, Hiai H. Persistent oxidative stress in cancer. *FEBS Lett*. 1995;358:1–3.
15. Thorpe PE. Vascular targeting agents as cancer therapeutics. *Clin Cancer Res*. 2004;10:415–427.
16. Zhao D, Stafford JH, Zhou H, Thorpe PE. Near-infrared optical imaging of exposed phosphatidylserine in a mouse glioma model. *Transl Oncol*. 2011;4:355–364.
17. Judy BF, Aliperti LA, Predina JD, et al. Vascular endothelial-targeted therapy combined with cytotoxic chemotherapy induces inflammatory intratumoral infiltrates and inhibits tumor relapses after surgery. *Neoplasia*. 2012;14:352–359.
18. Moody MA, Liao HX, Alam SM, et al. Anti-phospholipid human monoclonal antibodies inhibit CCR5-tropic HIV-1 and induce beta-chemokines. *J Exp Med*. 2010;207:763–776.
19. Jennewein M, Lewis MA, Zhao D, et al. Vascular imaging of solid tumors in rats with a radioactive arsenic-labeled antibody

that binds exposed phosphatidylserine. *Clin Cancer Res*. 2008;14:1377–1385.

20. Sullivan LA, Carbon JG, Roland CL, et al. r84, a novel therapeutic antibody against mouse and human VEGF with potent anti-tumor activity and limited toxicity induction. *PLoS One*. 2010;5:e12031.
21. Ran S, He J, Huang X, Soares M, Scothorn D, Thorpe PE. Antitumor effects of a monoclonal antibody directed against anionic phospholipids on the surface of tumor blood vessels in mice. *Clin Cancer Res*. 2005;11:1551–1562.
22. Ufret-Vincenty RL, Aredo B, Liu X, et al. Transgenic mice expressing variants of complement factor H develop AMD-like retinal findings. *Invest Ophthalmol Vis Sci*. 2010;51:5878–5887.
23. Zhou Q, Gallagher R, Ufret-Vincenty R, Li X, Olson EN, Wang S. Regulation of angiogenesis and choroidal neovascularization by members of microRNA-23∼27∼24 clusters. *Proc Natl Acad Sci U S A*. 2011;17:8287–8292.
24. Campa C, Kasman I, Ye W, Lee WP, Fuh G, Ferrara N. Effects of an anti-VEGF-A monoclonal antibody on laser-induced choroidal neovascularization in mice: optimizing methods to quantify vascular changes. *Invest Ophthalmol Vis Sci*. 2008;49:1178–1183.
25. Rohrer B, Coughlin B, Bandyopadhyay M, Holers VM. Systemic human CR2-targeted complement alternative pathway inhibitor ameliorates mouse laser-induced choroidal neovascularization. *J Ocul Pharmacol Ther*. 2012;28:402–409.
26. Rohrer B, Long Q, Coughlin B, et al. A targeted inhibitor of the alternative complement pathway reduces angiogenesis in a mouse model of age-related macular degeneration. *Invest Ophthalmol Vis Sci*. 2009;50:3056–3064.
27. Tomida D, Nishiguchi KM, Kataoka K, et al. Suppression of choroidal neovascularization and quantitative and qualitative inhibition of VEGF and CCL2 by heparin. *Invest Ophthalmol Vis Sci*. 2011;52:3193–3199.
28. Lu H, Lu Q, Gaddipati S, et al. IKK2 inhibition attenuates laser-induced choroidal neovascularization. *PLoS One*. 2014;9:e87530.
29. Aredo B, Zhang K, Chen X, Wang CXZ, Li T, Ufret-Vincenty RL. Differences in the distribution, phenotype and gene expression of subretinal microglia in C57BL/6N (Crb1rd8/rd8) vs. C57BL6/J (Crb1wt/wt) mice. *J Neuroinflammation*. 2015;12:6.
30. Shao Z, Friedlander M, Hurst CG, et al. Choroid sprouting assay: an ex vivo model of microvascular angiogenesis. *PLoS One*. 2013;8:e69552.
31. Yin Y, Huang X, Lynn KD, Thorpe PE. Phosphatidylserine-targeting antibody induces M1 macrophage polarization and promotes myeloid-derived suppressor cell differentiation. *Cancer Immunol Res*. 2013;1:256–268.
32. He J, Luster TA, Thorpe PE. Radiation-enhanced vascular targeting of human lung cancers in mice with a monoclonal antibody that binds anionic phospholipids. *Clin Cancer*. 2007;13:5211–5218.
33. DeRose P, Thorpe PE, Gerber DE. Development of bavituximab, a vascular targeting agent with immune-modulating properties, for lung cancer treatment. *Immunotherapy*. 2011;3:933–944.
34. She H, Li X, Yu W. Subthreshold transpupillary thermotherapy of the retina and experimental choroidal neovascularization in a rat model. *Graefes Arch Clin Exp Ophthalmol*. 2006;244:1143–1151.
35. Schmitz-Valckenberg S, Guo L, Maass A, et al. Real-time in vivo imaging of retinal cell apoptosis after laser exposure. *Invest Ophthalmol Vis Sci*. 2008;49:2773–2780.
36. Giani A, Thanos A, Roh MI, et al. In vivo evaluation of laser-induced choroidal neovascularization using spectral-domain optical coherence tomography. *Invest Ophthalmol Vis Sci*. 2011;52:3880–3887.
37. Liu T, Hui L, Wang YS, et al. In-vivo investigation of laser-induced choroidal neovascularization in rat using spectral-domain optical coherence tomography (SD-OCT). *Graefes Arch Clin Exp Ophthalmol*. 2013;251:1293–1301.
38. Berglin L, Sarman S, van der Ploeg I, et al. Reduced choroidal neovascular membrane formation in matrix metalloproteinase-2-deficient mice. *Invest Ophthalmol Vis Sci*. 2003;44:403–408.
39. Schick PK, Kurica KB, Chacko GK. Location of phosphatidylethanolamine and phosphatidylserine in the human platelet plasma membrane. *J Clin Invest*. 1976;57:1221–1226.
40. Bevers EM, Comfurius P, van Rijn JL, Hemker HC, Zwaal RF. Generation of prothrombin-converting activity and the exposure of phosphatidylserine at the outer surface of platelets. *Eur J Biochem*. 1982;122:429–436.
41. Fadok VA, Voelker DR, Campbell PA, Cohen JJ, Bratton DL, Henson PM. Exposure of phosphatidylserine on the surface of apoptotic lymphocytes triggers specific recognition and removal by macrophages. *J Immunol*. 1992;148:2207–2216.
42. Koopman G, Reutelingsperger CP, Kuijten GA, Keehnen RM, Pals ST, van Oers MH. Annexin V for flow cytometric detection of phosphatidylserine expression on B cells undergoing apoptosis. *Blood*. 1994;84:1415–1420.
43. Cordeiro MF, Migdal C, Bloom P, Fitzke FW, Moss SE. Imaging apoptosis in the eye. *Eye (Lond)*. 2011;25:545–553.
44. Herrmann A, Devaux PF. Alteration of the aminophospholipid-translocase activity during in vivo and artificial aging of human erythrocytes. *Biochim Biophys Acta*. 1990;1027:41–46.
45. Jemielity S, Wang JJ, Chan YK, et al. TIM-family proteins promote infection of multiple enveloped viruses through virion-associated phosphatidylserine. *PLoS Pathog*. 2013;9:e1003232.
46. Morohoshi K, Patel N, Ohbayashi M, et al. Serum autoantibody biomarkers for age-related macular degeneration and possible regulators of neovascularization. *Exp Mol Pathol*. 2012;92:64–73.
47. Cho-Chung YS. Autoantibody biomarkers in the detection of cancer. *Biochim Biophys Acta*. 2006;1762:587–591.
48. Defresne F, Bouzin C, Guilbaud C, et al. Differential influence of anticancer treatments and angiogenesis on the seric titer of autoantibody used as tumor and metastasis biomarker. *Neoplasia*. 2010;12:562–570.
49. Lu H, Ladd J, Feng Z, et al. Evaluation of known oncoantibodies, HER2, p53, and cyclin B1, in prediagnostic breast cancer sera. *Cancer Prev Res (Phila)*. 2012;5:1036–1043.
50. Liu R, Li X, Gao W, et al. Monoclonal antibody against cell surface GRP78 as a novel agent in suppressing PI3K/AKT signaling, tumor growth, and metastasis. *Clin Cancer Res*. 2013;19:6802–6811.
51. Goldhirsch A, Gelber RD, Piccart-Gebhart MJ, et al. 2 years versus 1 year of adjuvant trastuzumab for HER2-positive breast cancer (HERA): an open-label, randomised controlled trial. *Lancet*. 2013;382:1021–1028.
52. Huang X, Bennett M, Thorpe PE. A monoclonal antibody that binds anionic phospholipids on tumor blood vessels enhances the antitumor effect of docetaxel on human breast tumors in mice. *Cancer Res*. 2005;65:4408–4416.
53. Digumarti R, Bapsy PP, Suresh AV, et al. Bavituximab plus paclitaxel and carboplatin for the treatment of advanced non-small-cell lung cancer. *Lung Cancer*. 2014;86:231–236.
54. Kwak N, Okamoto N, Wood JM, Campochiaro PA. VEGF is major stimulator in model of choroidal neovascularization. *Invest Ophthalmol Vis Sci*. 2000;41:3158–3164.

Investigative Ophthalmology & Visual Science

55. Saishin Y, Saishin Y, Takahashi K, et al. VEGF-TRAP(R1R2) suppresses choroidal neovascularization and VEGF-induced breakdown of the blood-retinal barrier. *J Cell Physiol*. 2003; 195:241–248.

56. Apte RS, Richter J, Herndon J, Ferguson TA. Macrophages inhibit neovascularization in a murine model of age-related macular degeneration. *PLoS Med*. 2006;3:e310.

57. Liu J, Copland DA, Horie S, et al. Myeloid cells expressing VEGF and arginase-1 following uptake of damaged retinal pigment epithelium suggests potential mechanism that drives the onset of choroidal angiogenesis in mice. *PLoS One*. 2013; 8:e72935.

58. Silva RA, Moshfeghi AA, Kaiser PK, Singh RP, Moshfeghi DM. Radiation treatment for age-related macular degeneration. *Semin Ophthalmol*. 2011;26:121–130.

59. Comfurius P, Senden JM, Tilly RH, et al. Loss of membrane phospholipid asymmetry in platelets and red cells may be associated with calcium-induced shedding of plasma membrane and inhibition of aminophospholipid translocase. *Biochim Biophys Acta*. 1990;1026:153–160.

60. Zhou Q, Zhao J, Stout JG, Luhm RA, Wiedmer T, Sims PJ. Molecular cloning of human plasma membrane phospholipid scramblase. A protein mediating transbilayer movement of plasma membrane phospholipids. *J Biol Chem*. 1997;272: 18240–18244.

Investigative Ophthalmology & Visual Science